Downloaded from orbit.dtu.dk on: May 05, 2023

DTU Library

Double-P1 calculation of gamma-ray transport in semi-infinite media

Kirkegaard, P.

Publication date:
1972

Document Version
Publisher's PDF, also known as Version of record

Link back to DTU Orbit

Citation (APA):
Kirkegaard, P. (1972). *Double-P_1 calculation of gamma-ray transport in semi-infinite media*. Risø-M No. 1460

General rights
Copyright and moral rights for the publications made accessible in the public portal are retained by the authors and/or other copyright owners and it is a condition of accessing publications that users recognise and abide by the legal requirements associated with these rights.

- Users may download and print one copy of any publication from the public portal for the purpose of private study or research.
- You may not further distribute the material or use it for any profit-making activity or commercial gain
- You may freely distribute the URL identifying the publication in the public portal

If you believe that this document breaches copyright please contact us providing details, and we will remove access to the work immediately and investigate your claim.

A. E. K. Risø

Risø - M - 1460

Risø - M - 1460

Title and author(s)

Double-P_1 Calculation of Gamma-Ray Transport in Semi-Infinite Media

by P. Kirkegaard

Date April, 1972

Department or group

Reactor Physics Dept.

Group's own registration number(s)

27 pages + 1 tables + 6 illustrations

Abstract

A double-P_1 calculation method for γ-ray transport in semi-infinite and homogeneous media is outlined. The medium is adjacent to vacuum and contains γ-sources of a spatially uniform, but arbitrary spectral distribution. Particular attention is paid to calculation of the surface flux. The one-dimensional energy and angular-dependent transport equation is solved by an adaption of Gerstl's method. A short description is given of the computer program GAMP1.

Copies to

Standard distribution

125 copies

Abstract to

Available on request from the Library of the Danish Atomic Energy Commission (Atomenergikommissionens Bibliotek), Risø, Roskilde, Denmark.
Telephone: (03) 35 51 01, ext. 334, telex: 5072.

Fi 25-204

ISBN 87 550 0126 2

CONTENTS

1. INTRODUCTION

The aim of this report is to present a solution method for the γ-ray transport problem illustrated in fig. 1.

This problem has arisen in connection with calibration of γ-spectrometer measurements of the abundances of uranium, thorium, and potassium in a geologic formation containing these elements [1]. The volume-distributed γ-sources arise from the natural decay series of U, Th, and K in secular equilibrium.

When the spectrum of the source is known, and the γ scattering and absorption cross-sections for the medium are known as function of energy, it is possible to find the γ-flux throughout the medium, and in particular at the surface.

Several methods could, in principle, be used to solve this problem, e. g. Monte Carlo, spherical-harmonics (P_L) technique, and the moments method. As the geometry is one-dimensional, Monte-Carlo will certainly be inferior to an analytical method. Moments methods and standard P_L technique will run into difficulties in predicting the angular flux near the surface. The best choice seems to be the double-P_L method, where the upward and downward fluxes ($\omega < 0$ and $\omega > 0$ in fig. 1) are treated separately. Gerstl [2] has developed a variant of this method for finite slabs; the present work is to a wide extent based on his ideas.

2. FORMULATION OF THE TRANSPORT PROBLEM

The general Boltzmann equation for stationary photon transport reads [3, 4]

$$\nabla \cdot \Omega N(r, \Omega, E) + \mu(r, E)\, N(r, \Omega, E) =$$

$$\int\int_{4\pi} N(r, \Omega', E')\, \sigma(r, \Omega' \to \Omega, E' \to E) dE'\, d\Omega' + s(r, \Omega, E) \quad . \qquad (1)$$

N is the angular and differential number flux of photons. μ is the total macroscopic cross section and σ the transference cross section; it is assumed that the photon interactions are either absorptions or Compton scatterings, which is nearly true [3] in the energy range of interest to us (0.1 - 3 MeV). r, Ω are position and direction vectors, and E is energy. Values prior to collision are indicated by dashes. As the medium is assumed homo-

geneous, μ and σ do not depend on r. In the following (1) will be recast into a form more convenient for computations [3].

First we introduce the energy flux $I = EN$ instead of the number flux N:

$$\nabla \cdot \Omega I + \mu I = \int\int_{4\pi} I(r, \Omega', E')\, \sigma(\Omega' \to \Omega, E' \to E)\, \frac{E}{E'}\, dE'\, d\Omega' + Es(r, \Omega, E) \quad . \tag{2}$$

Next, we replace E by the Compton wavelength

$$\lambda = \frac{f}{E} \tag{3}$$

($f = 0.51083$, E in MeV, λ in Compton units). From Compton's formula

$$1 - \Omega \cdot \Omega' = \frac{f}{E} - \frac{f}{E'} = \lambda - \lambda' \tag{4}$$

we find that the transference cross section σ becomes

$$\sigma(\Omega' \to \Omega, E' \to E) = \frac{d\sigma}{d\Omega}\, \delta(1 + \lambda' - \lambda - \Omega \cdot \Omega')\, \frac{d\lambda}{dE} \quad , \tag{5}$$

where $\frac{d\sigma}{d\Omega} = \int \sigma(\Omega' \to \Omega, E' \to E)\, dE$ is the differential angle cross section.

Withe these substitutions (2) becomes

$$\nabla \cdot \Omega I(r, \Omega, \lambda) + \mu(\lambda)\, I(r, \Omega, \lambda) =$$

$$\int\int_{4\pi} I(r, \Omega', \lambda')\, \frac{\lambda}{\lambda'}\, \frac{d\sigma}{d\Omega}\, \delta(1 + \lambda' - \lambda - \Omega \cdot \Omega')\, d\Omega'\, d\lambda' + Es(r, \Omega, \lambda) \quad . \tag{6}$$

Notice that I and s in (6) are still measured per energy unit, just as in (2) (not per wavelength unit). From a numerical point of view (6) is more attractive than (2) because as a rule $I(r, \Omega, \lambda)$ is a smoother function of λ than is $N(r, \Omega, E)$ of E.

$\frac{d\sigma}{d\Omega}$ is given by the Klein - Nishina formula [4]

$$\frac{d\sigma}{d\Omega} = n_e\, \sigma_o\, \frac{3}{16\pi}\, \frac{\lambda'^2}{\lambda^2} \left(\frac{\lambda}{\lambda'} + \frac{\lambda'}{\lambda} - \sin^2\theta \right), \tag{7}$$

where n_e is the electronic density, σ_o (= 0.6653 barns/electron) the Thomson cross section, and $\cos\theta = \Omega \cdot \Omega'$. From (4) we have

$$\frac{d\sigma}{d\Omega} = \frac{1}{2\pi} \frac{\lambda'}{\lambda} k(\lambda', \lambda) \quad , \tag{8}$$

where the kernel k is defined as

$$k(\lambda', \lambda) = n_e \sigma_o \frac{3}{8} \frac{\lambda'}{\lambda} \left(\frac{\lambda}{\lambda'} + \frac{\lambda'}{\lambda} - 2(\lambda - \lambda') + (\lambda - \lambda')^2 \right) \tag{9}$$

if $\lambda' \leq \lambda \leq \lambda' + 2$ and otherwise as 0.

Insertion in (6) yields

$$\nabla \cdot \Omega I + \mu I = \int_{\lambda-2}^{\lambda} \int_{4\pi} I(r, \Omega', \lambda') \, k(\lambda', \lambda) \, \frac{\delta(1+\lambda'-\lambda-\Omega\cdot\Omega')}{2\pi} \, d\Omega' \, d\lambda' +$$

$$Es(r, \Omega, \lambda) \quad . \tag{10}$$

This equation specialized to our one-dimensional case (fig. 1) becomes

$$\omega \frac{\partial I}{\partial x} + \mu(\lambda) I = \int_{\lambda-2}^{\lambda} \int_{4\pi} I(x, \omega', \lambda') \, k(\lambda', \lambda) \, \frac{\delta(1+\lambda'-\lambda-\Omega\cdot\Omega')}{2\pi} \, d\Omega' \, d\lambda' + \tag{11}$$

$$\frac{Eq(\lambda)}{4\pi} \quad . \qquad\qquad (x \geq 0)$$

The source $s(r, \Omega, \lambda)$ has been written $\frac{q(\lambda)}{4\pi}$ because it is assumed isotropic and independent of position; $q(\lambda)$ is the source strength in photons/MeV/cm^3/s.

Now, the energy flux I may be split into an uncollided part U and a scattered part Ψ :

$$I(x, \omega, \lambda) = U(x, \omega, \lambda) + \Psi(x, \omega, \lambda) \tag{12}$$

The direct flux U is easily calculated to be

$$U(x, \omega, \lambda) = \begin{cases} p(\lambda) \left[1 - \exp\left(- \frac{\mu(\lambda) x}{\omega} \right) \right], & 0 < \omega \leq 1 \\ p(\lambda) \quad , & -1 \leq \omega < 0 \quad . \end{cases} \tag{13}$$

The coefficient $p(\lambda)$ stems from the source and is given by

$$p(\lambda) = \frac{Eq(\lambda)}{4\pi\mu(\lambda)} \quad . \tag{14}$$

From (11) the equation for Ψ is obtained:

$$\omega \frac{\partial \Psi(x,\omega,\lambda)}{\partial x} + \mu(\lambda)\,\Psi(x,\omega,\lambda) =$$

$$\int_{\lambda-2}^{\lambda} \int_{4\pi} [\Psi(x,\omega',\lambda') + U(x,\omega',\lambda')]\, k(\lambda',\lambda)\, \frac{\delta(1+\lambda'-\lambda-\Omega\cdot\Omega')}{2\pi}\, d\Omega'\, d\lambda'$$

$$(x \geq 0) \quad . \tag{15}$$

The scattered flux Ψ obtained from (15) may be expected to behave more regularly than the total flux I obtained from (11).

The boundary conditions for (15) pertaining to our case (fig. 1) are:

(a) no downward flux at the surface $x = 0$:

$$\Psi(0,\omega,\lambda) = 0\,, \quad 0 < \omega \leq 1 \tag{16}$$

and (b) finite flux for $x \to \infty$:

$$\Psi(\infty,\omega,\lambda) < \infty \tag{17}$$

3. DERIVATION OF THE DOUBLE-P_1 EQUATIONS

Gerstl[2] points out that the boundary condition (16) induces step properties in the solution at $\omega = 0$, and suggests that $\Psi(\omega < 0)$ and $\Psi(\omega > 0)$ should be treated differently with a separate spherical-harmonic expansion for each. We define

$$\Psi^{\pm}(x,\omega,\lambda) = \Psi(x,\omega,\lambda)\, H(\pm\omega) \quad , \tag{18}$$

$$U^{\pm}(x,\omega,\lambda) = U(x,\omega,\lambda)\, H(\pm\omega) \quad , \tag{19}$$

where $H(\omega) = \begin{cases} 0 & \text{for } \omega < 0 \\ 1 & \omega > 0 \end{cases}$ is the Heaviside step function.

Then for all ω, $\Psi = \Psi^+ + \Psi^-$ and $U = U^+ + U^-$, and (15) becomes

$$\omega \frac{\partial \Psi^{\pm}(x,\omega,\lambda)}{\partial x} + \mu(\lambda)\, \Psi^{\pm}(x,\omega,\lambda) = \int_{\lambda-2}^{\lambda} \int_{4\pi} (\Psi^+(x,\omega',\lambda') + U^+ + \Psi^- + U^-)\, k(\lambda',\lambda)\, \frac{\delta(1+\lambda'-\lambda-\Omega\cdot\Omega')}{2\pi}\, d\Omega'\, d\lambda' \,, \tag{20}$$

U^+ and U^- being given by (13) and (19). The boundary conditions are now

$$\left.\begin{aligned} &\Psi^+(0,\omega,\lambda) = 0 \\ &\lim_{x\to\infty} \Psi^{\pm}(x,\omega,\lambda) = \Psi_\infty(\lambda) < \infty \end{aligned}\right\} \tag{21}$$

the isotropic deep-limit flux $\Psi_\infty(\lambda)$ satisfies the equation

$$\mu(\lambda)\cdot\Psi_\infty(\lambda) = \int_{\lambda-2}^{\lambda} \int_{4\pi} \left\{\Psi_\infty(\lambda') + p(\lambda')\right\} k(\lambda',\lambda)\, \frac{\delta(1+\lambda'-\lambda-\omega\cdot\omega')}{2\pi}\, d\Omega'\, d\lambda' \,. \tag{22}$$

The components of (20) are expanded in half-range spherical harmonics. In the range $0 < \omega < 1$ the expansion

$$\varphi(\omega) = \sum_{l=0}^{\infty} (2l+1)\, a_l\, P_l(2\omega-1), \quad a_l = \int_0^1 \varphi(\omega)\, P_l(2\omega-1)\, d\omega \,, \tag{23}$$

and in $-1 < \omega < 0$ the expansion

$$\varphi(\omega) = \sum_{l=0}^{\infty} (2l+1)\, a_l\, P_l(2\omega+1), \quad a_l = \int_{-1}^{0} \varphi(\omega)\, P_l(2\omega+1)\, d\omega \tag{24}$$

are used. Making the abbreviations [2]

$$P_l^{\pm}(\omega) = P_l(2\omega \mp 1)\, H(\pm\omega) \,, \quad \int^{+} = \int_0^1 \,, \text{ and } \int^{-} = \int_{-1}^{0} \,, \text{ we find}$$

$$\Psi^{\pm}(x,\omega,\lambda) = \sum_{l=0}^{\infty} (2l+1)\, \Psi_l^{\pm}(x,\lambda)\, P_l^{\pm}(\omega)\,,$$

$$\Psi^{\pm}(x,\lambda) = \int^{+} \Psi(x,\omega,\lambda)\, P_l^{\pm}(\omega)\, d\omega \qquad (25)$$

and

$$U^{\pm}(x,\omega,\lambda) = \sum_{l=0}^{\infty} (2l+1)\, U_l^{\pm}(x,\lambda)\, P_l^{\pm}(\omega)\,,$$

$$U_l^{\pm}(x,\lambda) = \int^{\pm} U(x,\omega,\lambda)\, P_l^{\pm}(\omega)\, d\omega \qquad (26)$$

The scattering kernel is expanded in full-range spherical harmonics in $\Omega\cdot\Omega'$. If we write $\Omega\cdot\Omega' = \omega\omega' + \sqrt{1-\omega^2}\ \sqrt{1-\omega'^2}\cos(\varphi-\varphi')$, so that φ and φ' are azimuthal angles of Ω and Ω', we may apply the addition theorem for Legendre polynomials [6]; apart from sign we get

$$\frac{\delta(1+\lambda'-\lambda-\Omega\cdot\Omega')}{2\pi} = \sum_{n=0}^{\infty} \sum_{m=-n}^{n} \frac{2n+1}{4\pi} P_n(1+\lambda'-\lambda)\,(-1)^m\, P_n^m(\omega')\, P_n^{-m}(\omega)$$

$$\exp\left[\,im(\varphi-\varphi')\,\right]\,. \qquad (27)$$

Insertion of these expressions in (20) yields

$$\omega \sum_{l=0}^{\infty} (2l+1)\, \frac{\partial\, \Psi_l^{\pm}(x,\lambda)}{\partial x}\, P_l^{\pm}(\omega) + \mu(\lambda) \sum_{l=0}^{\infty} (2l+1)\, \Psi_l^{\pm}(x,\lambda)\, P_l^{\pm}(\omega) =$$

$$\int_{\lambda-2}^{\lambda} k(\lambda',\lambda) \int_{4\pi} \sum_{l=0}^{\infty} (2l+1) \left[(\Psi_l^{+}(x,\lambda') + U_l^{+})\, P_l^{+}(\omega') + (\Psi_l^{-}+U_l^{-})\, P_l^{-}(\omega') \right] \times$$

$$\times \sum_{n=0}^{\infty} \sum_{m=-n}^{n} \frac{2n+1}{4\pi} P_n(1+\lambda'-\lambda)(-1)^m\, P_n^m(\omega')\, P_n^{-m}(\omega)\, e^{im(\varphi-\varphi')}\, d\Omega'\, d\lambda' \qquad (28)$$

A reduction of (28) is obtained by use of the recursion and orthogonality relations for $P_l^{\pm}(\omega)$ (see the Appendix). The first member of (28) is written

$$\sum_{l=0}^{\infty} (2l+1) \left\{ \frac{1}{2(2l+1)} \frac{\partial \Psi_{l-1}^{\pm}(x,\lambda)}{\partial x} \pm \frac{1}{2} \frac{\partial \Psi_{l}^{\pm}}{\partial x} + \frac{l+1}{2(2l+1)} \frac{\partial \Psi_{l+1}^{\pm}}{\partial x} + \right.$$

$$\left. + \mu(\lambda) \Psi_l^{\pm} \right\} P_l^{\pm}(\omega)$$

In the second member we put $d\Omega' = d\omega' \, d\varphi'$ and integrate first with respect to φ' and then with respect to ω'. The result is

$$\int_{\lambda-2}^{\lambda} k(\lambda', \lambda) \sum_{l=0}^{\infty} \sum_{n=0}^{\infty} \frac{2l+1}{2} (2n+1) \, P_n(1+\lambda'-\lambda) \, P_n(\omega) \left[(\Psi_l^{+}(x,\lambda') + U_l^{+}) c_{nl}^{+} + \right.$$

$$\left. + (\Psi_l^{-} + U_l^{-}) c_{nl}^{-} \right] d\lambda'$$

(the coefficients $c_{nl}^{\pm} = \int_{-}^{+} P_n(\omega) \, P_l^{\pm}(\omega) d\omega$ are discussed in the Appendix).

This is now expanded in $P_l^{\pm}(\omega)$; using $P_n(\omega) = \sum_{l=0}^{\infty} (2l+1) c_{nl}^{\pm} P_l^{\pm}(\omega)$,

we obtain finally an expression, in which the coefficient to $(2l+1)P_l^{\pm}(\omega)$ is equalled to that for the first member of (28). The resulting equation is

$$\frac{1}{2(2l+1)} \frac{\partial \Psi_{l-1}^{\pm}}{\partial x} \pm \frac{1}{2} \frac{\partial \Psi_{l}^{\pm}}{\partial x} + \frac{l+1}{2(2l+1)} \frac{\partial \Psi_{l+1}^{\pm}}{\partial x} + \mu(\lambda) \Psi_l^{\pm} =$$

$$\sum_{n=i}^{\infty} \frac{2n+1}{2} c_{nl}^{\pm} \int_{\lambda-2}^{\lambda} k(\lambda', \lambda) \, P_n(1+\lambda'-\lambda) \sum_{l'=0}^{n} (2l'+1) \left[(\Psi_{l'}^{+}(x,\lambda') + U_{l'}^{+}) c_{nl'}^{+} + \right.$$

$$\left. + (\Psi_{l'}^{-} + U_{l'}^{-}) c_{nl'}^{-} \right] d\lambda' \qquad (29)$$

as

$$U_{l'}^{+} c_{nl'}^{+} + U_{l'}^{-} c_{nl'}^{-} = p(\lambda') \left\{ c_{nl'}^{+} \int_{0}^{1} P_{l'}^{+}(\omega) \left[1 - \exp\left(- \frac{\mu(\lambda')x}{\omega} \right) \right] d\omega + \right.$$

$$\left. + c_{nl'}^{-} \int_{-1}^{0} P_{l'}^{-}(\omega) \, d\omega \right\} = p(\lambda') \left[2\delta_{no} \delta_{l'o} - c_{nl'}^{+} V_{l'}(\mu' x) \right]$$

($\mu' \equiv \mu(\lambda')$, and $V_l(y) = \int_{0}^{1} P_l^{+}(\omega) \exp\left(-\frac{y}{\omega}\right) d\omega$, cf. the Appendix),

(29) may be written

$$\frac{1}{2(2l+1)}\frac{\partial \Psi^{\pm}_{l-1}(x,\lambda)}{\partial x} \pm \frac{1}{2}\frac{\partial \Psi^{\pm}_{l}}{\partial x} + \frac{l+1}{2(2l+1)}\frac{\partial \Psi^{\pm}_{l+1}}{\partial x} + \mu(\lambda)\,\Psi^{\pm}_{l} =$$

$$\delta_{lo}\int_{\lambda-2}^{\lambda} k(\lambda',\lambda)\,p(\lambda')\,d\lambda' + \sum_{n=1}^{\infty}\frac{2n+1}{2}\,c^{\pm}_{nl}\int_{\lambda-2}^{\lambda} k(\lambda',\lambda)\,P_n(1+\lambda'-\lambda)$$

$$\sum_{l'=0}^{n}(2l'+1)\left[\left(\Psi^{+}_{l'}(x,\lambda') - p(\lambda')\,V_{l'}(\mu' x)\right)c^{+}_{nl'} + \Psi^{-}_{l'}(x,\lambda')c^{-}_{nl'}\right]d\lambda' \tag{30}$$

Henceforward we shall be concerned with the consistent double-P_1 approximation, i.e. we require $\forall l > 1$: $\Psi^{\pm}_{l} = V_l = 0$. Then (30) reduces to four coupled differential equations:

$$\frac{1}{2}\frac{\partial}{\partial x}\left(\pm\Psi^{\pm}_{o}(x,\lambda) + \Psi^{\pm}_{1}(x,\lambda)\right) + \mu(\lambda)\,\Psi^{\pm}_{o}(x,\lambda) = \int_{\lambda-2}^{\lambda} k(\lambda',\lambda)\,p(\lambda')\,d\lambda' +$$

$$\sum_{n=0}^{\infty}\frac{2n+1}{2}\,c^{\pm}_{no}\int_{\lambda-2}^{\lambda} P_n(1+\lambda'-\lambda)\,k(\lambda',\lambda)\sum_{l=0}^{1}(2l+1)\left[c^{+}_{nl}\left(\Psi^{+}_{l}(x,\lambda') - \right.\right.$$

$$\left.\left. p(\lambda')\,V_l(\mu' x)\right) + c^{-}_{nl}\,\Psi^{-}_{l}(x,\lambda')\right]d\lambda' \tag{31}$$

$$\frac{1}{6}\frac{\partial}{\partial x}\left(\Psi^{\pm}_{o}(x,\lambda) \pm 3\Psi^{\pm}_{1}(x,\lambda)\right) + \mu(\lambda)\,\Psi^{\pm}_{1}(x,\lambda) =$$

$$\sum_{n=1}^{\infty}\frac{2n+1}{2}\,c^{\pm}_{n1}\int_{\lambda-2}^{\lambda} P_n(1+\lambda'-\lambda)\,k(\lambda',\lambda)\sum_{l=0}^{1}(2l+1)\left[c^{+}_{nl}\left(\Psi^{+}_{l}(x,\lambda') - \right.\right.$$

$$\left.\left. - p(\lambda')\,V_l(\mu' x)\right) + c^{-}_{nl}\,\Psi^{-}_{l}(x,\lambda')\right]d\lambda' \tag{32}$$

The source will now be taken to be a line spectrum

$$q(\lambda) = \sum_{p=1}^{p} Q_p\,\delta(E-E_p) \tag{33}$$

The spectrum has P lines, and Q_p is the intensity in photons/cm^3/s of line no. p with energy E_p and wavelength $\lambda_s^p = k/E_p$. According to (14) we have for an arbitrary function $G(\lambda',\lambda)$

$$\int_{\lambda-2}^{\lambda} G(\lambda',\lambda)p(\lambda')\,d\lambda' = \sum_p \frac{\lambda_s^p Q_p}{4\pi\mu_s^p} G(\lambda_s^p,\lambda)$$

The summation is extended over lines in the integration interval from $\lambda-2$ to λ. Thus the systems (31)-(32) becomes equivalent to

$$\begin{bmatrix} \frac{1}{2} & \frac{1}{2} & 0 & 0 \\ \frac{1}{6} & \frac{1}{2} & 0 & 0 \\ 0 & 0 & -\frac{1}{2} & \frac{1}{2} \\ 0 & 0 & \frac{1}{6} & -\frac{1}{2} \end{bmatrix} \frac{\partial}{\partial x} \begin{bmatrix} \Psi_o^+(x,\lambda) \\ \Psi_1^+(x,\lambda) \\ \Psi_o^-(x,\lambda) \\ \Psi_1^-(x,\lambda) \end{bmatrix} + \mu(\lambda) \begin{bmatrix} \Psi_o^+(x,\lambda) \\ \Psi_1^+(x,\lambda) \\ \Psi_o^-(x,\lambda) \\ \Psi_1^-(x,\lambda) \end{bmatrix} =$$

$$\int_{\lambda-2}^{\lambda} k(\lambda',\lambda) \begin{bmatrix} A & 3C & B & 3D \\ C & 3E & -D & 3F \\ B & -3D & A & -3C \\ D & 3F & -C & 3E \end{bmatrix}_{\lambda-\lambda'} \begin{bmatrix} \Psi_o^+(x,\lambda') \\ \Psi_1^+(x,\lambda') \\ \Psi_o^-(x,\lambda') \\ \Psi_1^-(x,\lambda') \end{bmatrix} d\lambda' +$$

$$+ \sum_p \frac{\lambda_s^p Q_p\, k(\lambda_s^p,\lambda)}{4\pi\mu_s^p} \left\{ \begin{bmatrix} 1 \\ 0 \\ 1 \\ 0 \end{bmatrix} - \begin{bmatrix} A & 3C \\ C & 3E \\ B & -3D \\ D & 3F \end{bmatrix}_{-\lambda-\lambda_s^p} \cdot \begin{bmatrix} V_o(\mu_s^p x) \\ V_1(\mu_s^p x) \end{bmatrix} \right\} \quad (34)$$

The coefficients A, B, C, D, E, F, which depend on $\lambda-\lambda'$ (or $\lambda-\lambda_s^p$), are equal to sums of the type

$s(a_n, \beta_n) = \sum_{n=0}^{\infty} \frac{2n+1}{2} P_n(1+\lambda'-\lambda)\, a_n \beta_n$; in fact we have

$A = s(c_{no}^+, c_{no}^+)$, $B = s(c_{no}^+, c_{no}^-)$, $C = s(c_{no}^+, c_{n1}^+)$, $D = s(c_{no}^+, c_{n1}^-)$, $E = s(c_{n1}^+, c_{n1}^+)$, and $F = s(c_{n1}^+, c_{n1}^-)$. They are further discussed in the Appendix and in sec. 5. If (34) is premultiplied by the matrix

$$\begin{bmatrix} 3 & -3 & 0 & 0 \\ -1 & 3 & 0 & 0 \\ 0 & 0 & -3 & -3 \\ 0 & 0 & -1 & -3 \end{bmatrix} ,$$

the result is

$$\frac{\partial}{\partial x} \begin{bmatrix} \Psi_o^+(x,\lambda) \\ \Psi_1^+(x,\lambda) \\ \Psi_o^-(x,\lambda) \\ \Psi_1^-(x,\lambda) \end{bmatrix} = \mu(\lambda) \begin{bmatrix} -3 & 3 & 0 & 0 \\ 1 & -3 & 0 & 0 \\ 0 & 0 & 3 & 3 \\ 0 & 0 & 1 & 3 \end{bmatrix} \begin{bmatrix} \Psi_o^+(x,\lambda) \\ \Psi_1^+(x,\lambda) \\ \Psi_o^-(x,\lambda) \\ \Psi_1^-(x,\lambda) \end{bmatrix} +$$

$$\int_{\lambda-2}^{\lambda} k(\lambda',\lambda) \begin{bmatrix} a & b & c & d \\ e & f & g & h \\ -c & d & -a & b \\ g & -h & e & -f \end{bmatrix}_{\lambda-\lambda'} \begin{bmatrix} \Psi_o^+(x,\lambda') \\ \Psi_1^+(x,\lambda') \\ \Psi_o^-(x,\lambda') \\ \Psi_1^-(x,\lambda') \end{bmatrix} d\lambda' +$$

$$+ \sum_p \frac{\lambda_s^p Q_p\, k(\lambda_s^p, \lambda)}{4\pi \mu_s^p} \left\{ \begin{bmatrix} 3 \\ -1 \\ -3 \\ -1 \end{bmatrix} - \begin{bmatrix} a & b \\ e & f \\ -c & d \\ g & -h \end{bmatrix}_{\lambda-\lambda_s^p} \cdot \begin{bmatrix} V_o(\mu_s^p x) \\ V_1(\mu_s^p x) \end{bmatrix} \right\} \quad (35)$$

with a = 3A-3C, b = 9C-9E, c = 3B+3D, d = 9D-9F, e = -A+3C, f = -3C+9E, g = -B-3D, and h = -3D+9F.

4. SOLUTION OF THE EQUATIONS

In this section we shall consider the numerical solution of (35). The two variables of the problem, λ and x, are treated differently: the wavelength will be discretized and integration over λ approximated by summation, while the integration of the equations with respect to x will be treated by an analytical, though not exact, method.

Let E_{max} be the highest energy in the source spectrum, and let the energy range of interest go down to some cut-off value E_{cut}. A wavelength mesh is constructed by taking $\lambda_{min} = f/E_{max}$ and selecting a step size $\Delta\lambda$ such that $1/\Delta\lambda = m$ is integral (fig. 2). λ_{max} and the number of intervals, N, are chosen such that $\lambda_{max} = \lambda_{min} + N\Delta\lambda$ is approximately equal to f/E_{cut}. Use of a single step length $\Delta\lambda$ for the whole range from λ_{min} to λ_{max} is not always economical. This choice was made, however, because in the actual applications the range has been rather narrow, and the set-up and coding are simpler for fixed $\Delta\lambda$.

A complication arises because the solution Ψ of (35) for fixed x, say $x = \infty$, has discontinuities induced by the source lines; line no. p causes one jump in Ψ at $\lambda = \lambda_s^p$ and another one at $\lambda = \lambda_s^p + 2$ (fig. 2). Altogether 2P jumps occur, and we shall at these points calculate both the limit from the left, $\Psi(\lambda-0)$, and the jump $\Psi(\lambda+0) - \Psi(\lambda-0)$.

The discrete counterpart to (35) is

$$\frac{d}{dx}\begin{bmatrix} \Psi^+_{oi} \\ \Psi^+_{1i} \\ \Psi^-_{oi} \\ \Psi^-_{1i} \end{bmatrix} = \mu_i \begin{bmatrix} -3 & 3 & 0 & 0 \\ 1 & -3 & 0 & 0 \\ 0 & 0 & 3 & 3 \\ 0 & 0 & 1 & 3 \end{bmatrix} \begin{bmatrix} \Psi^+_{oi} \\ \Psi^+_{1i} \\ \Psi^-_{oi} \\ \Psi^-_{1i} \end{bmatrix} +$$

$$\sum_{j=i-m}^{i} \xi_{ij}\, k_{ji} \begin{bmatrix} a & b & c & d \\ e & f & g & h \\ -c & d & -a & b \\ g & -h & e & -f \end{bmatrix}_{i-j} \begin{bmatrix} \Psi_{oj}^{+} \\ \Psi_{1j}^{+} \\ \Psi_{oj}^{-} \\ \Psi_{1j}^{-} \end{bmatrix} \Delta\lambda +$$

$$\sum_{p} \frac{\lambda_{j_p} Q_p k_{j_p i}}{4\pi\mu_{j_p}} \left\{ \begin{bmatrix} 3 \\ -1 \\ -3 \\ -1 \end{bmatrix} - \begin{bmatrix} a & b \\ e & f \\ -c & d \\ g & -h \end{bmatrix}_{i-j_p} \cdot \begin{bmatrix} V_{oj_p} \\ V_{1j_p} \end{bmatrix} \right\} \qquad (36)$$

Index i refers to the wavelength $\lambda_i = \lambda_{min} + (i-1)\Delta\lambda$ $(1 \leq i \leq N+1)$. For brevity we have written k_{ji} for $k(\lambda_j, \lambda_i)$, μ_i for $\mu(\lambda_i)$, $\Psi_{li}^{\pm}$ for $\Psi_l^{\pm}(x, \lambda_i)$, and V_{li} for $V_l(\mu_i x)$. The source term is obtained by moving each source line λ_s^p to the nearest wavelength mesh point j_p (several lines may be represented by the same mesh point). The ξ_{ij} are suitably chosen quadrature weights (see the Appendix).

In the Appendix is shown that in the case $\lambda - \lambda' = 0$ $(i-j = 0)$ we have $A = 1$, $E = \frac{1}{3}$, $B = C = D = F = 0$, hence $a = 3$, $b = -3$, $e = -1$, $f = 3$, $c = d = g = h = 0$. This means that (36) is equivalent to the system

$$\frac{d}{dx} \begin{bmatrix} \Psi_o^{+} \\ \Psi_1^{+} \\ \Psi_o^{-} \\ \Psi_1^{-} \end{bmatrix} = \mu \begin{bmatrix} -3 & 3 & 0 & 0 \\ 1 & -3 & 0 & 0 \\ 0 & 0 & 3 & 3 \\ 0 & 0 & 1 & 3 \end{bmatrix} \begin{bmatrix} \Psi_o^{+} \\ \Psi_1^{+} \\ \Psi_o^{-} \\ \Psi_1^{-} \end{bmatrix} + \begin{bmatrix} \varphi_o^{+} \\ \varphi_1^{+} \\ \varphi_o^{-} \\ \varphi_1^{-} \end{bmatrix} \qquad (37)$$

with $\mu = \mu_i - \Delta\lambda\, \xi_{ii}\, k_{ii}$ (index i in the Ψ and φ is suppressed). Such a system exists for all the N+1 wavelength points in the range. It is now essential that we first solve (37) for the shortest wavelength (i = 1) and then for i = 2, i = 3, ..., i = N+1, in that order. In this way φ_o^{+}, φ_1^{+}, φ_o^{-}, and φ_1^{-}, which are derived from (36), will contain known functions only,

and (37) degenerates for each i into two independent systems I and II. Both of these are of the form

$$\Psi' = P\Psi + \varphi \tag{38}$$

and are treated in much the same way. The eigenvalues λ_1, λ_2 of the two-by-two matrix P is found, and also the eigenvector matrix A satisfying PA = AD with

$$D = \begin{bmatrix} \lambda_1 & 0 \\ 0 & \lambda_2 \end{bmatrix} .$$

The functional transformation $\Psi = A\chi$ is applied to (38), which is transformed into

$$\chi' = D\chi + h \tag{39}$$

with $h = A^{-1}\varphi$. The vector equation (39) is equivalent to the two scalar equations

$$\chi'_m(x) = \lambda_m \chi_m(x) + h_m(x), \quad m = 1, 2 \tag{40}$$

with the complete solutions

$$\chi_m(x) = \exp(\lambda_m x) \left\{ \int \exp(-\lambda_m x)\, h_m(x)\, dx + C_m \right\} \tag{41}$$

An exact analytical representation of $\chi_m(x)$ is very complicated, because the source term in our problem induces exponential integrals (cf. Appendix), and the complexity increases rapidly as the wavelength integration proceeds. We choose instead an approximative method. The physical nature of the problem indicates that $h_m(x)$ can be adequately represented by a decaying exponential multiplied by a polynomial in x, plus a constant:

$$h_m(x) = h_{mo} + \exp(a_m x) \sum_{j=1}^{k} h_{mj}\, x^{j-1} \qquad (a_m < 0) \tag{42}$$

h_{mo} is given by $h_o = A^{-1}\varphi_o$ with $\varphi_o = \lim_{x \to \infty} \varphi(x)$. The other parameters in (42) are determined in the least-squares sense, operating with a fixed mesh of x-values, so that the actual $h_m(x)$ is first calculated at the mesh points from lower-wavelength solution-values in the same mesh points. The

applied least-squares-fitting method is discussed in the Appendix. Insertion of (42) in (41) yields

$$\chi_m(x) = -\frac{h_{mo}}{\lambda_m} + C_m \exp(\lambda_m x) + \exp(\lambda_m x) \sum_{j=1}^{k} h_{mj} \int \exp((a_m-\lambda_m)x)\cdot x^{j-1}\, dx$$

or

$$\chi_m(x) = -\frac{h_{mo}}{\lambda_m} + C_m \exp(\lambda_m x) + \exp(a_m x) \sum_{j=1}^{k} \varkappa_{mj}\, x^{j-1} \quad , \qquad (43)$$

where $\varkappa_{mk} = \frac{1}{a_m-\lambda_m} h_{mk}$, $\varkappa_{mj} = \frac{1}{a_m-\lambda_m} (h_{mj}-j\cdot \varkappa_{m,j+1})$,

$$j = k-1, \ldots, 1 \ .$$

From this point we shall treat case I and case II separately.

Case I

$$P = \mu \begin{bmatrix} -3 & 3 \\ 1 & -3 \end{bmatrix}$$

The eigenvalues are $\lambda_1 = -\mu(3 + \sqrt{3})$ and $\lambda_2 = -\mu(3 - \sqrt{3})$; both are negative.

The eigenvector matrix is

$$A = \begin{bmatrix} \sqrt{3} & \sqrt{3} \\ -1 & 1 \end{bmatrix} \quad , \quad \text{and} \quad A^{-1} = \begin{bmatrix} \frac{1}{2\sqrt{3}} & -\frac{1}{2} \\ \frac{1}{2\sqrt{3}} & \frac{1}{2} \end{bmatrix} \quad .$$

The boundary condition (cf. (21)) is $\Psi(0) = 0$; or, as $\chi = A^{-1}\Psi$, $\chi(0) = 0$. With this condition (43) gives

$$C_m = \frac{h_{mo}}{\lambda_m} - \varkappa_{m1} \ , \text{ and}$$

$$\chi_m(x) = -\frac{h_{mo}}{\lambda_m} + \left(\frac{h_{mo}}{\lambda_m} - \varkappa_{m1}\right) \exp(\lambda_m x) + \exp(a_m x) \sum_{j=1}^{k} \varkappa_{mj}\, x^{j-1} \ ;$$

(44)

finally $\Psi = A\chi$ is calculated.

Case II

$$P = \mu \begin{bmatrix} 3 & 3 \\ 1 & 3 \end{bmatrix}$$

The eigenvalues are $\lambda_1 = \mu(3 + \sqrt{3})$ and $\lambda_2 = \mu(3 - \sqrt{3})$; both are positive.

The eigenvector matrix is

$$A = \begin{bmatrix} \sqrt{3} & \sqrt{3} \\ 1 & -1 \end{bmatrix}, \text{ and } A^{-1} = \begin{bmatrix} \frac{1}{2\sqrt{3}} & \frac{1}{2} \\ \frac{1}{2\sqrt{3}} & -\frac{1}{2} \end{bmatrix}$$

The boundary condition (cf. (21)) is $\Psi(\infty) < \infty$; or, as $\chi = A^{-1}\Psi$, $\chi(\infty) < \infty$.

With this condition (43) gives $C_m = 0$, and

$$\chi_m(x) = -\frac{h_{mo}}{\lambda_m} + \exp(a_m x) \sum_{j=1}^{k} \varkappa_{mj} x^{j-1} \; ; \qquad (45)$$

finally $\Psi = A\chi$ is calculated.

5. THE COMPUTER PROGRAM GAMP1 WITH INPUT DESCRIPTION

A FORTRAN program GAMP1 (Danish AEC program no. 648) was written along the lines of the previous sections. It is primarily intended to be run on a Burroughs B6700, but should be operable on other computers with little change.

5.1. Structure of the Program

GAMP1 consists of a driver program (MAIN), and the subprograms GAMP, DATAIO, AMYG, AW, AH, E2, WQUADR, AKERNL, EXPPOL, COLDEC, and COLSOL. In order to utilize the fast memory most efficiently, variable dimensions are used; the array bounds are passed from the driver program to the master subroutine GAMP which governs the flow of the calculations, see the flow diagram in fig. 3. The other subprograms

are discussed below.

5.2. Description of Subprograms

DATAIO is a subroutine that reads input data from punched cards, prints out these data, and passes them to the main program.

AMYG is a function subprogram with the arguments IZ (atomic no.) and E (energy in MeV). It calculates the total γ-cross-section (Compton + photo + pair) for an element in cm^2/g according to NBS prescriptions [8]. Table 1 contains cross sections calculated by AMYG for the same elements and energies as those given in Goldstein pp. 235-36 [4]. The agreement is quite acceptable, apart from the range with heavy elements at low energies. It is the intention later on to improve on this by replacing AMYG by a routine which reads from some basic γ-cross-section library tape.*

AW is a block-data subprogram. It causes the atomic-weight table to be compiled into labelled common storage for use in MAIN and AMYG.

AH is a subroutine that calculates the coefficients a, b, ..., h in (35) and (36). These numbers (see (35), (34), and the Appendix) are linear combinations of A(γ), ..., F(γ), which in turn are given as infinite series:

$$A(\gamma) = \sum_{n=0}^{\infty} \frac{2n+1}{2} c_{no}^2 P_n(\gamma) ,$$

and similar expressions for the others. They are to be calculated for a set of discrete and equidistant γ-values in the interval $-1 \leq \gamma \leq 1$ (as $\gamma = 1 + \lambda' - \lambda$ and $\lambda' \leq \lambda \leq \lambda' + 2$). From (A13)-(A18) it appeared sufficient to calculate directly only A(γ) and E(γ) and only for $\gamma \geq 0$. In his paper, Gerstl [2] operates with series of a nature similar to ours, also containing P_n. He points out that the partial sum of such series,

$$s_N = \sum_{n=0}^{N} a_n ,$$

converges only slowly to the limit s as $N \to \infty$, but that $s - s_N$ for large N fluctuates regularly around zero. In fact, the average

$$\bar{s}_N = \frac{1}{6} \sum_{m=1}^{6} s_{N-m+1}$$

---

* Note added in proof: This improvement has now been made; the data tape used is the Livermore Evaluated Photon Interaction Library (HPIC, DLC-7D, ENDF/B file 23)

has proved to approach s quite fast. In the present subroutine $\tilde{s}_{200}$ is used as an approximation to s; c_{no}, c_{n1}, and $P_n(\gamma)$ are calculated by successive application of the appropriate recursion relations.

E2 is a function subprogram with the argument X. It calculates the second-order exponential integral

$$E_2(x) = x \int_x^\infty \frac{\exp(-t)}{t^2}\, dt \qquad \text{for} \quad x \geq 0.$$

The values of E2 were compared to Placzek's table reproduced in Goldstein pp. 358-65 [4]. In no case was found a deviation of more than one on the least significant decimal place.

WQUADR is a subroutine that calculates the quadrature weights in (A19) for arbitrary values m (= $j_2 - j_1 + 1$) of the number of quadrature points. The formulas are given in the Appendix.

AKERNL is a function subprogram with arguments ALMD and ALM (λ' and λ). It calculates the variable factor of the scattering kernel (9) viz.

$$k(\lambda',\lambda)/(\frac{3}{8}\, n_e \sigma_o) = \frac{\lambda'}{\lambda}\left(\frac{\lambda}{\lambda'} + \frac{\lambda'}{\lambda} - 2(\lambda-\lambda') + (\lambda'-\lambda)^2\right).$$

EXPPOL is a subroutine that carries out the least-squares fitting discussed in the Appendix.

COLDEC and COLSOL are subroutines to be used in the solution of systems of linear equations with positive-definite matrices, as they occur in EXPPOL. The two routines belong to the Danish AEC Library of FORTRAN Subprograms at Risø (SF/148).

5.3. Preparation of Input Data for GAMP1

Problem no. (IPNO), format I10. IPNO < 0 terminates the job stream.

Headline (HEADL), format 12A6. Descriptive text.

Punch option (IPCH), format I10. IPCH = 0 means that the output appears only on lineprinter. If IPCH = 1, it appears both on lineprinter and as punched cards (for further processing).

Density (RHO), format E10.5. In g/cm^3 for the homogeneous mixture.

Number of elements (NMAT), format I10.

Atomic no. and partial wgtpct. for element no. N in the mixture (the order is irrelevant) (IZN(N), WPCT(N)), format I10, E10.5. Altogether NMAT cards must be punched.

Number of source lines (LINNUM), format I10. Restriction LINNUM ≤ 25.

Source energies (ESOUR(IS), IS = 1, LINNUM), format 8E10.5 (the order is irrelevant). In MeV.

Source strengths (YIELD(IS), IS = 1, LINNUM), format 8E10.5, same order as the source energies. Expressed in photons/s/decaying atom.

Lower energy cut-off (ECUT), format E10.5. In MeV.

Wavelength division (MLAM), format I10. MLAM is the number of subintervals into which the Compton wavelength unit is divided.

Space division (NX), format I10. NX is the number of space mesh points including infinity and the surface point. Restriction: NX ≤ 20.

Degree of fit (KM1), format I10. KM1 is the degree of the polynomials used in the least-squares fit. Restriction KM1 ≤ 7. Recommendation: KM1 = 2.

Input data for a sample problem (cf. sec. 6) are reproduced in the Appendix, together with the corresponding sample output.

6. EXPERIENCE WITH THE PROGRAM

All the subroutines of GAMP1 were checked in separate test runs, and so was the complete program. Besides these debugging tests, a large number of trial runs were executed to investigate the various approximations in the model. It was concluded that sufficient accuracy (error ≤ about 0.1 percent on the flux) is obtained provided

(a) N = 200 is used in $\bar{s}_N$ (cf. description of AH in subsection 5.2); this N is fixed in the program and not available to the user,
(b) MLAM (cf. subsection 5.3) ≥ 128,
(c) NX (cf. subsection 5.3) ≥ 9,
(d) KM1 (cf. subsection 5.3) ≥ 2.

Fig. 4 shows a comparison between deep-flux results obtained by GAMP1 and by a Monte Carlo program. There is a significant difference

between the shapes of the two spectra, but this might be due to the fact that the rule for picking scattered wavelengths in the Monte Carlo program was only approximately correct.

Figs. 5 and 6 show graphical representations of GAMP1 results as obtained by processing the punched output with a simple plotter program. The example refers to a case with practical importance: calculation of the γ-spectrum above concrete containing sources from the natural-uranium decay series in secular equilibrium. These plots suggest that the (Ψ,λ)-representation is the better of the two from a computational point of view (cf. sec. 2). The small 1st harmonic component indicates that the double-P_1 approximation is adequate for problems of this type. The sample input/output print-out in the Appendix refers to this GAMP1 problem.

The computer time for the sample problem was 50 s (CPU-time) on the B-6700. The use of variable dimensions (subsection 5.1) proved to imply considerable gain in efficiency.

7. SUMMARY AND CONCLUSIONS

The present report has presented a double-P_1 transport-theory model for calculation of the γ-spectrum above a semi-infinite medium with sources, and a computer program GAMP1 has been described. In our view the selected method represents a reasonable compromise between efficiency and accuracy.

The results are intended to form the basis of calibration calculations involving the response of scintillation detectors.

There is some interest in a future extension of the GAMP1 model in which the vacuum would be replaced by a homogeneous medium, in particular air.

8. REFERENCES

1) L. Løvborg et al., Field Determination of Uranium and Thorium by Gamma-Ray Spectrometry, Exemplified by Measurements in the Ilimaussaq Alkaline Intrusion, South Greenland. Econ. Geol., v. 66 (1971) 368-384.

2) S. A. W. Gerstl, An Improved Double P_L Method Applied to Gamma Transport. Nukleonik 8 (1966) 101-108.

3) H. Goldstein and J. E. Wilkins, Jr., Calculation of the Penetration of Gamma Rays. Final Report. NYO-3075 (1954) 203 pp.

4) H. Goldstein, Fundamental Aspects of Reactor Shielding. (Addison-Wesley Publishing Co., Reading, Mass., USA, 1959). 416 pp.

5) P. Kirkegaard, Some Aspects of the General Least-Squares Problem for Data Fitting. Risø-M-1399 (1971). 16 pp.

6) E. T. Whittaker and G. N. Watson, A Course of Modern Analysis, 4th edition. (University Press, Cambridge, 4, 1952). 608 pp.

7) C.-E. Fröberg, Lärobok i numerisk analys. (Bonniers, Stockholm, 1962). 277 pp.

8) G. White Grodstein, X-Ray Attenuation Coefficients from 10 keV to 100 MeV. (NBS Circular, 583). USGPO, Washington D. C., 1957). 54 pp.

9) L. Løvborg, private communication.

9. ACKNOWLEDGEMENT

The author is indebted to G. K. Kristiansen who proposed the double-P_L technique for solution of the problem.

APPENDIX

The Polynomials $P_l^{\pm}(\omega)$

From the definition $P_l^{\pm}(\omega) = P_l(2\omega^2 - 1)\, H(\pm\omega)$ $(l = 0, 1, 2, \ldots)$ and the recurrence relation for $P_l(\omega)$,

$$\omega P_l(\omega) = \frac{l+1}{2l+1} P_{l+1}(\omega) + \frac{l}{2l+1} P_{l-1}(\omega),$$

the following recurrence formula is obtained:

$$\pm P_l^{\pm}(\omega) = 2\omega P_l^{\pm}(\omega) - \frac{l+1}{2l+1} P_{l+1}^{\pm}(\omega) - \frac{l}{2l+1} P_{l-1}^{\pm}(\omega) \qquad (A1)$$

The orthogonality relations are

$$\int_{-1}^{+1} P_l^{\pm}(\omega)\, P_m^{\pm}(\omega)\, d\omega = \frac{1}{2l+1} \delta_{lm} \qquad (A2)$$

The Coefficients $c_{nl}^{\pm}$ [2)]

From the definition $c_{nl}^{\pm} = \int_{-1}^{+1} P_n(\omega)\, P_l^{\pm}(\omega)\, d\omega$, some elementary properties are deduced:

$$c_{no}^{+} + c_{no}^{-} = 2\delta_{no}, \qquad (A3)$$

$$c_{nl}^{-} = (-1)^{n+1} c_{nl}^{+}; \qquad (A4)$$

hence only c_{nl}^{+} need be considered (the superscript + is dropped in the following);

$$\forall l > n : c_{nl} = 0, \qquad (A5)$$

$$c_{2\nu,o} = \delta_{\nu o}, \qquad (A6)$$

$$c_{2\nu-1,o} = \frac{(-1)^{\nu-1}(2\nu)!}{2^{2\nu}(2\nu-1)(\nu!)^2}, \qquad (A7)$$

(cf. ref. 6 p. 306). (A6) and (A7) give a convenient calculation procedure for c_{no}:

$$c_{oo} = 1, \quad c_{1o} = \frac{1}{2}, \quad c_{no} = -\frac{n-2}{n+1} c_{n-2,o}, \quad n = 2, 3, 4, \ldots \tag{A8}$$

It may be shown that c_{n1} can be calculated from

$$c_{n1} = \frac{2}{n+2} c_{n-1,o} - c_{no} . \tag{A9}$$

Finally we shall prove that

$$\sum_{n=0}^{\infty} \frac{2n+1}{2} c_{nl}^2 = \frac{1}{2l+1} . \tag{A10}$$

We define a function $Y_l(\omega)$, $-1 < \omega < 1$:

$$Y_l(\omega) = \begin{cases} 0 , & -1 < \omega < 0 \\ P_l^+(\omega) , & 0 < \omega < 1 , \end{cases}$$

and expand it in spherical harmonics, $Y_l(\omega) = \sum_{n=0}^{\infty} a_{nl} P_n(\omega)$ with

$$a_{nl} = \frac{2n+1}{2} \int_0^1 P_l^+(\omega) P_n(\omega) \, d\omega = \frac{2n+1}{2} c_{nl} .$$

But from (A2) we obtain

$$\frac{1}{2l+1} = \int_{-1}^{1} [Y_l(\omega)]^2 \, d\omega = \sum_{n=0}^{\infty} a_{nl}^2 \frac{2}{2n+1} = \sum_{n=0}^{\infty} \frac{2n+1}{2} c_{nl}^2 ,$$

and thus (A10) is verified.

The Integrals V_l

The source-induced integrals $V_l(y) = \int_0^1 P_l^+(\omega) \exp\left(-\frac{y}{\omega}\right) d\omega$

can be expressed in terms of the exponential integral

$$E_2(y) = y \int_y^{\infty} \frac{\exp(-t)}{t^2} \, dt .$$

For $l = 0$ and 1 we find

$$V_0(y) = E_2(y) \tag{A11}$$

$$V_1(y) = \exp(-y) - (1+y)\, E_2(y) \tag{A12}$$

The Coefficients A, B, C, D, E, F

These figures were defined after eq. (34); they are functions of $\lambda-\lambda'$, or, which is the same, of the parameter $\gamma = 1 + \lambda' - \lambda$. It is easily shown that there are the following relations between them:

$$A(\gamma) + B(\gamma) = 1 \tag{A13}$$

$$C(\gamma) - D(\gamma) = 0 \tag{A14}$$

$$E(\gamma) + F(\gamma) = \frac{1}{3}\gamma - 2C(\gamma) \tag{A15}$$

$$A(\gamma) + C(\gamma) = \frac{1}{2} + \frac{1}{2}\gamma \tag{A16}$$

Once A and E are calculated, the others follow from these formulas. Further, it is only necessary to compute $A(\gamma)$ and $E(\gamma)$ for $\gamma \geq 0$ owing to the relations

$$A(-\gamma) = 1 - A(\gamma) \tag{A17}$$

$$E(-\gamma) = 1 + \frac{2}{3}\gamma - 2A(\gamma) + E(\gamma) \tag{A18}$$

For $\gamma = 1$ we find $A(1) = \sum_{n=0}^{\infty} \frac{2n+1}{2} c_{no}^{+2}$ and $E(1) = \sum_{n=0}^{\infty} \frac{2n+1}{2} c_{n1}^{+2}$;

(A10) gives immediately $A(1) = 1$ and $E(1) = \frac{1}{3}$, whereafter (A13-16) give $B(1) = 0$, $C(1) = 0$, $D(1) = 0$, and $F(1) = 0$.

Numerical Quadrature

(35) contains integrals which in (36) were replaced by sums,

$$\int_{\lambda_1}^{\lambda_2} F(\lambda)\, d\lambda \simeq \sum_{j=j_1}^{j_2} w_j\, F(\lambda_j)\, \Delta\lambda \tag{A19}$$

we shall in particular be concerned with the quadrature weights w_j (ξ_{ij} in

(36)). The integrand may have discontinuities in the interval considered; such points will be taken as boundaries between different quadrature ranges for evaluation of the sum of the right which breaks into parts representing intervals of continuity (for a discontinuity point, w_j will be the sum of two terms). In (A19) we may hereafter suppose that $F(\lambda)$ is continuous, and we shall state the applied quadrature rules with the associated weights w_j. The formula chosen depends on the number of intervals $n = j_2 - j_1$, as specified below.

n	Quadrature rule	Quadrature weights
1	Trapezoidal	$w_{j_1} = w_{j_2} = \frac{1}{2}$
3	Cote's 3rd order [7]	$w_{j_1} = w_{j_2} = \frac{3}{8}$, $w_{j_1+1} = w_{j_2-1} = \frac{9}{8}$
even	Simpson	$w_{j_1} = w_{j_2} = \frac{1}{3}$, $w_{j_1+1} = w_{j_1+3} = \ldots = w_{j_2-1} = \frac{4}{3}$, $w_{j_1+2} = w_{j_1+4} = \ldots = w_{j_2-2} = \frac{2}{3}$
odd, > 3	Cote's 3rd order for the short-wavelength part, Simpson for the remaining	Combination of the two types above

Least-Squares Fit

We shall consider the determination of the coefficients in the expression (42) for $h_m(x)$.

From the beginning, a fixed set of discrete x-values, $x_1, x_2, \ldots, x_n$, was chosen such that $\exp(-cx_i) = 1 - (i-1)/n$; the transformation parameter c should be taken equal to a typical γ-cross-section value for the actual energy range, e. g. the geometrical mean between the extreme cross-section values.

The function $h_m(x)$ is well defined (although it might have come out from fitting procedures at lower wavelengths), and the values $h_m(x_i)$ can be calculated. The constant term h_{mo} in (42) could be found analytically; hence the problem we face is to find a set of parameters $\{a_1, \ldots, a_{k_1}, \beta\}$ that makes the function

$$\left.\begin{aligned} f(x) &= \sum_{j=1}^{k} a_j \varphi_j(x_i;\ \beta) \\ \text{with}\quad \varphi_j(x_i\ \beta) &\equiv \exp(\beta x)\cdot x^{j-1} \end{aligned}\right\} \qquad \text{(A20)}$$

at $\{x_1, \ldots, x_n\}$ take on values $\{f_1, \ldots, f_n\}$ that are as close as possible to the prescribed ordinates $\{y_1, \ldots, y_n\}$ ($y_i = h_m(x_i) - h_{mo}$). A least-squares fit is obtained by requiring that

$$\Phi = \sum_{i=1}^{n} w_i(y_i - f_i)^2 \qquad \text{(A21)}$$

must be minimum. w_i are the weights of the data points (x_i, y_i) (they will here be taken to be unity). We use the semi-linear method described in ref. 5. In this method, Marquardt iterations are performed in the non-linear space, which in our case is the one-dimensional β-space. The linear space is k-dimensional (cf. (42)) with points $a = (a_1, \ldots, a_k)^T$. The controlling equation $(A + \lambda D^2)\,\delta\beta = g$ [5] for Marquardt iterations specializes to

$$\delta\beta = \frac{g}{a(1+\lambda)} \qquad \text{(A22)}$$

with $a = \sum_i w_i \left(\frac{\partial f_i}{\partial \beta}\right)^2$ and $g = \sum_i w_i(y_i - f_i)\frac{\partial f_i}{\partial \beta}$. The linear part of the problem will be, given a β (guessed or iterated), to find the a-vector that minimizes Φ. This a is a solution to the kth order linear system

$$C\,a = \gamma \qquad \text{(A23)}$$

with

$$c_{j,j_1} = \sum_i w_i \varphi_j \varphi_{j_1} = \sum_i w_i \exp(\beta x_i)\, x_i^{j-1} \exp(\beta x_i)\, x_i^{j_1-1}$$

and

$$\gamma_j = \sum_i w_i y_i \varphi_j = \sum_i w_i y_i \exp(\beta x_i)\, x_i^{j-1}.$$

The derivative $\frac{\partial f_i}{\partial \beta}$ to be used to form (A22) has the value

$$\frac{\partial f_i}{\partial \beta} = \sum_{j=1}^{k}\left[\frac{\partial \alpha_j}{\partial \beta}\, \varphi_j + \alpha_j \frac{\partial \varphi_j}{\partial \beta}\right] = \sum_{j}\left[\frac{\partial \alpha_j}{\partial \beta} \exp(\beta x_i)\, x_i^{j-1} + \alpha_j\, x_i \exp(\beta x_i)\, x_i^{j-1}\right] =$$

$$x_i\, f_i + \exp(\beta x_i) \sum_{j} \frac{\partial \alpha_j}{\partial \beta}\, x_i^{j-1} \ ,$$

where $d = \left(\frac{\partial \alpha_1}{\partial \beta}, \ldots, \frac{\partial \alpha_k}{\partial \beta} \right)^T$ satisfies the linear system

$$C\,d = t \quad \text{with} \quad t_j = \sum_{i} w_i \left[(y_i - f_i) \frac{\partial \varphi_j}{\partial \beta} - \varphi_j \sum_{j_1=1}^{k} \alpha_{j_1} \frac{\partial \varphi_{j_1}}{\partial \beta} \right]$$

$$= \sum_{i} w_i (y_i - 2f_i) \exp(\beta x_i)\, x_i^j \ .$$

Input Data for Sample Problem

```
PRINT-OUT OF GAMP1 DATA FOR SAMPLE PROBLEM

          1
CONCRETE/U    RISOE STANDARD
          1
2.0
         11
          1       0.23
          8      53.01
         11       0.27
         12       0.13
         13       1.48
         14      34.57
         19       0.52
         20       9.35
         22       0.09
         25       0.02
         26       0.33
         13
2.43      2.20      2.12      1.90      1.76      1.73      1.51      1.42
1.38      1.28      1.24      1.16      1.12
0.02      0.06      0.01      0.03      0.19      0.02      0.03      0.04
0.06      0.02      0.07      0.02      0.20
1.
        128
          9
          2
         -1
```

Output for Sample Problem

```
PROBLEM NO    1

CONCRETE/U    RISOE STANDARD

OPTION FOR PUNCHED-CARD OUTPUT =    1

DENSITY =     2.0000

NUMBER OF MATERIALS =  11

      COMPOSITION
ATOMIC NO      WGTPCT
      1         0.2300
      8        53.0100
     11         0.2700
     12         0.1300
     13         1.4800
     14        34.5700
     19         0.5200
     20         9.3500
     22         0.0900
     25         0.0200
     26         0.3300

SUMPCT =   100.0000


SOURCE LINE SPECTRUM WITH  13 LINES

ENERGY(MEV)     PHOTONS PER DECAYING ATOM
     2.4300                0.0200
     2.2000                0.0600
     2.1200                0.0100
     1.9000                0.0300
     1.7600                0.1900
     1.7300                0.0200
     1.5100                0.0300
     1.4200                0.0400
     1.3800                0.0600
     1.2800                0.0200
     1.2400                0.0700
     1.1600                0.0200
     1.1200                0.2000

CUTOFF ENERGY =      1.0000 MEV

NUMBER OF STEPS PER COMPTON WAVELENGTH = 128

NUMBER OF SPACE INTEGRATION POINTS (INFINITY INCLUDED) =    9

DEGREE OF POLYNOMIAL USED IN FIT =    2

WORKING STORAGE DEMAND =    3261
```

AVERAGE ATOMIC NO = 11.3658

ELECTRONS PER CM3 * E-24 = 0.6022

TRANSFORMATION PARAMETER C = 0.1017

40 ENERGY GROUPS

THE FLUXES BELOW ARE DIFFERENTIAL AND DIRECTIONAL
SCATTERED GAMMA ENERGY FLUXES PER UNIT VOLUME RATE OF DECAY
AT POINTS OF DISCONTINUITY THE SHORT-WAVELTH LIMIT IS GIVEN

GROUP NO	ENERGY (MEV)	COMPTON WAVELTH	MU-TOTAL (1/CM)	MU-SCAT (1/CM)	DEEP FLUX	SURFACE FLUX	1.HARMONIC IN DBLE-P1
1	2.430000	0.210218	0.081010	0.078721	0.000000	0.000000	0.000000
2	2.342928	0.218031	0.082529	0.080434	0.014815	0.014565	-0.000171
3	2.261880	0.225843	0.084025	0.082110	0.014364	0.014004	-0.000244
4	2.186252	0.233656	0.085500	0.083751	0.013960	0.013517	-0.000297
5	2.115517	0.241468	0.086954	0.085358	0.058116	0.056851	-0.000853
6	2.049217	0.249281	0.088389	0.086932	0.063994	0.062216	-0.001192
7	1.986946	0.257093	0.089804	0.088476	0.062401	0.060259	-0.001426
8	1.928347	0.264906	0.091199	0.089990	0.060956	0.058515	-0.001614
9	1.873106	0.272718	0.092575	0.091476	0.059642	0.056938	-0.001777
10	1.820942	0.280531	0.093932	0.092935	0.080713	0.077395	-0.002176
11	1.771605	0.288343	0.095270	0.094367	0.079103	0.075401	-0.002416
12	1.724870	0.296156	0.096591	0.095775	0.218632	0.212205	-0.004243
13	1.680538	0.303968	0.097895	0.097158	0.229046	0.221032	-0.005275
14	1.638428	0.311781	0.099182	0.098517	0.224657	0.215444	-0.006036
15	1.598376	0.319593	0.100452	0.099854	0.220615	0.210390	-0.006664
16	1.560236	0.327406	0.101707	0.101169	0.216886	0.205758	-0.007214
17	1.523874	0.335218	0.102945	0.102464	0.213443	0.201495	-0.007704
18	1.489167	0.343031	0.104169	0.103738	0.232510	0.219431	-0.008399
19	1.456007	0.350843	0.105377	0.104992	0.229150	0.215188	-0.008924
20	1.424291	0.358656	0.106571	0.106227	0.226037	0.211285	-0.009381
21	1.393928	0.366468	0.107750	0.107444	0.252813	0.236815	-0.010140
22	1.364832	0.374281	0.108915	0.108643	0.294119	0.276429	-0.011193
23	1.336925	0.382093	0.110067	0.109825	0.290406	0.271536	-0.011894
24	1.310138	0.389906	0.111205	0.110990	0.286951	0.267048	-0.012489
25	1.284402	0.397718	0.112330	0.112139	0.283732	0.264750	-0.011987
26	1.259658	0.405531	0.113442	0.113272	0.295566	0.275760	-0.012458
27	1.235850	0.413343	0.114541	0.114389	0.292540	0.271770	-0.012982
28	1.212925	0.421156	0.115628	0.115492	0.341652	0.319002	-0.014109
29	1.190834	0.428968	0.116703	0.116580	0.338256	0.314154	-0.014923
30	1.169535	0.436781	0.117766	0.117655	0.335082	0.309625	-0.015658
31	1.148983	0.444593	0.118818	0.118715	0.346960	0.319973	-0.016515
32	1.129142	0.452406	0.119858	0.119763	0.343976	0.315616	-0.017248
33	1.109974	0.460218	0.120886	0.120797	0.489736	0.457579	-0.019621
34	1.091446	0.468031	0.121904	0.121819	0.485163	0.450643	-0.020999
35	1.073526	0.475843	0.122911	0.122829	0.480865	0.444304	-0.022148
36	1.056185	0.483656	0.123907	0.123826	0.476823	0.438392	-0.023172
37	1.039396	0.491468	0.124893	0.124812	0.473022	0.432866	-0.024093
38	1.023132	0.499281	0.125869	0.125786	0.469446	0.427685	-0.024927
39	1.007369	0.507093	0.126834	0.126750	0.466087	0.422839	-0.025679
40	0.992085	0.514906	0.127789	0.127702	0.462931	0.418314	-0.026351

THE VALUES BELOW ARE THE JUMPS IN THE SCATTERED GAMMA ENERGY FLUXES

13 JUMPS IN THE SCATTERED FLUX

JUMP NO	GROUP NO	DEEP JUMP	SURFACE JUMP	1-HARMONIC JUMP
1	1	0.015320	0.015320	0.000000
2	4	0.046336	0.046336	-0.000000
3	5	0.007741	0.007741	-0.000000
4	9	0.023023	0.023023	0.000000
5	11	0.145532	0.145532	-0.000000
6	12	0.015368	0.015368	-0.000000
7	17	0.022865	0.022865	0.000000
8	20	0.030458	0.030458	0.000000
9	21	0.045787	0.045787	0.000000
10	25	0.015180	0.015180	0.000000
11	27	0.053100	0.053100	-0.000000
12	30	0.015175	0.015175	0.000000
13	32	0.151601	0.151601	0.000000

THE FLUXES BELOW ARE THE UNCOLLIDED PHOTON ENERGY FLUXES AT THE SURFACE
(MEV PER CM2 PER SEC PER STERAD PER UNIT VOLUME RATE OF DECAY)

GROUP NO	LINE NO	ADJUSTED ENERGY	SURFACE FLUX
1	1	2.430000	0.047740
4	2	2.186252	0.122088
5	3	2.115517	0.019360
9	4	1.873106	0.048304
11	5	1.771605	0.281159
12	6	1.724870	0.028421
17	7	1.523874	0.035339
20	8	1.424291	0.042541
21	9	1.393928	0.061768
25	10	1.284402	0.018198
27	11	1.235850	0.060102
30	12	1.169535	0.015806
32	13	1.129142	0.149935

Table 1

Total γ-cross-sections (cm^2/g) calculated by "AMYG"

MEV	H	BE	C	O	NA	AL
0.0100	0.3963	0.5575	2.2659	6.3132	18.8871	34.2603
0.0150	0.3768	0.2647	0.7117	1.7443	4.9905	9.0161
0.0200	0.3697	0.2014	0.3825	0.7744	2.0132	3.5697
0.0300	0.3572	0.1688	0.2294	0.3295	0.6444	1.0533
0.0400	0.3459	0.1581	0.1929	0.2310	0.3472	0.5063
0.0500	0.3356	0.1517	0.1778	0.1959	0.2474	0.3245
0.0600	0.3261	0.1467	0.1689	0.1788	0.2038	0.2468
0.0800	0.3091	0.1386	0.1575	0.1613	0.1670	0.1846
0.1000	0.2945	0.1319	0.1491	0.1511	0.1506	0.1598
0.1500	0.2651	0.1186	0.1337	0.1343	0.1301	0.1335
0.2000	0.2429	0.1087	0.1224	0.1227	0.1181	0.1201
0.3000	0.2112	0.0945	0.1064	0.1065	0.1021	0.1035
0.4000	0.1892	0.0847	0.0953	0.0954	0.0914	0.0925
0.5000	0.1728	0.0773	0.0870	0.0871	0.0834	0.0844
0.6000	0.1599	0.0715	0.0805	0.0806	0.0771	0.0780
0.8000	0.1404	0.0628	0.0707	0.0708	0.0677	0.0685
1.0000	0.1262	0.0565	0.0636	0.0636	0.0609	0.0615
1.5000	0.1026	0.0459	0.0517	0.0518	0.0496	0.0502
2.0000	0.0876	0.0393	0.0444	0.0445	0.0428	0.0434
3.0000	0.0691	0.0313	0.0356	0.0359	0.0348	0.0355
4.0000	0.0579	0.0266	0.0304	0.0309	0.0303	0.0311
5.0000	0.0502	0.0234	0.0270	0.0277	0.0274	0.0283
6.0000	0.0447	0.0211	0.0245	0.0253	0.0253	0.0263
8.0000	0.0371	0.0180	0.0212	0.0223	0.0227	0.0239
10.0000	0.0321	0.0160	0.0192	0.0205	0.0213	0.0226

MEV	SI	FE	SN	W	PB	U
0.0100	45.5819	305.1190	1316.9191	2062.9144	2133.3546	2102.2712
0.0150	12.0029	83.5011	396.7476	684.9845	731.7542	750.9844
0.0200	4.7323	33.3665	169.4383	313.3940	342.5943	361.8817
0.0300	1.3636	9.2415	51.1585	104.1983	117.6598	129.4357
0.0400	0.6299	3.7793	21.9317	47.7678	55.1867	62.4796
0.0500	0.3864	1.9305	11.4077	26.1248	30.7163	35.5538
0.0600	0.2830	1.1438	6.7134	15.9817	19.0569	22.4564
0.0800	0.2014	0.5412	2.9458	7.3966	9.0100	10.9135
0.1000	0.1701	0.3331	1.5847	4.0979	5.0680	6.2641
0.1500	0.1391	0.1787	0.5580	1.4444	1.8242	2.3266
0.2000	0.1244	0.1362	0.2967	0.7194	0.9132	1.1813
0.3000	0.1068	0.1057	0.1509	0.2999	0.3747	0.4841
0.4000	0.0954	0.0917	0.1082	0.1795	0.2175	0.2752
0.5000	0.0870	0.0827	0.0889	0.1292	0.1517	0.1868
0.6000	0.0804	0.0761	0.0777	0.1030	0.1177	0.1411
0.8000	0.0706	0.0665	0.0647	0.0768	0.0843	0.0967
1.0000	0.0635	0.0596	0.0568	0.0636	0.0680	0.0756
1.5000	0.0518	0.0488	0.0460	0.0490	0.0511	0.0546
2.0000	0.0448	0.0426	0.0410	0.0438	0.0454	0.0481
3.0000	0.0367	0.0362	0.0367	0.0403	0.0419	0.0441
4.0000	0.0323	0.0330	0.0354	0.0399	0.0415	0.0436
5.0000	0.0296	0.0314	0.0353	0.0406	0.0423	0.0444
6.0000	0.0275	0.0292	0.0293	0.0255	0.0229	0.0189
8.0000	0.0252	0.0284	0.0314	0.0303	0.0287	0.0258
10.0000	0.0239	0.0284	0.0336	0.0348	0.0339	0.0320

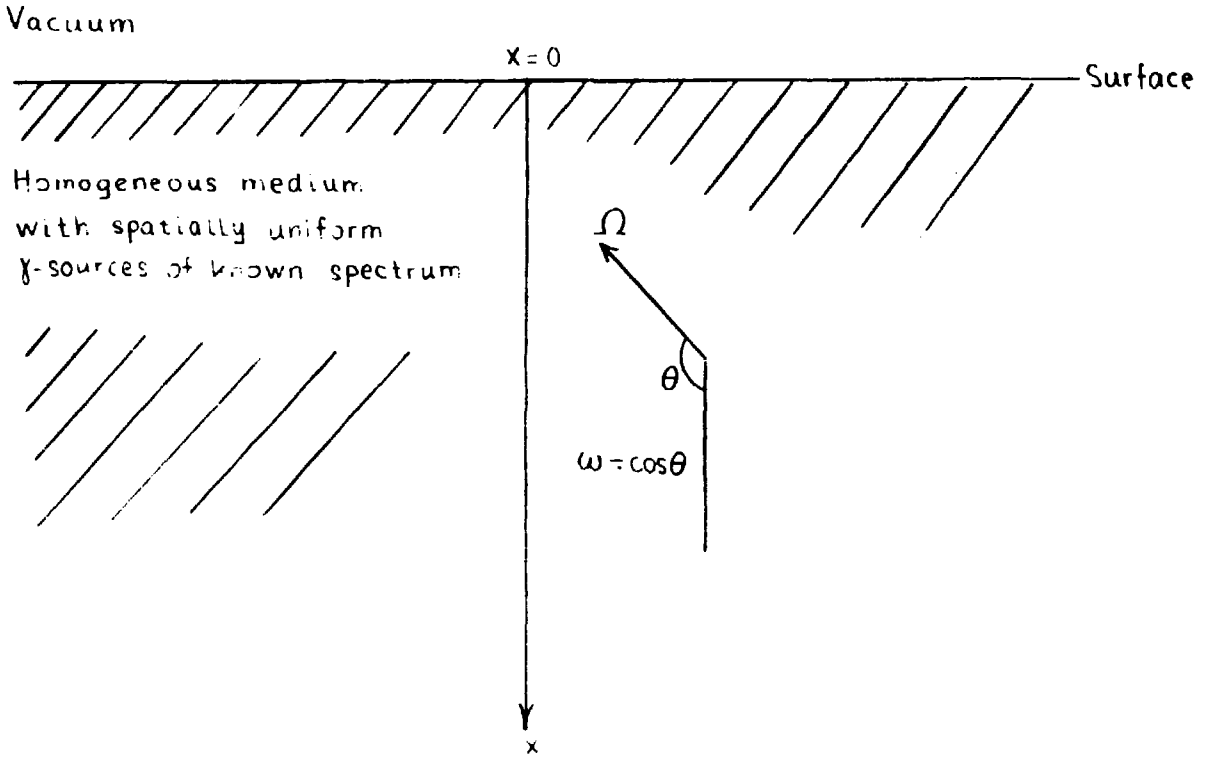

Fig. 1. Geometry for the gamma transport problem.

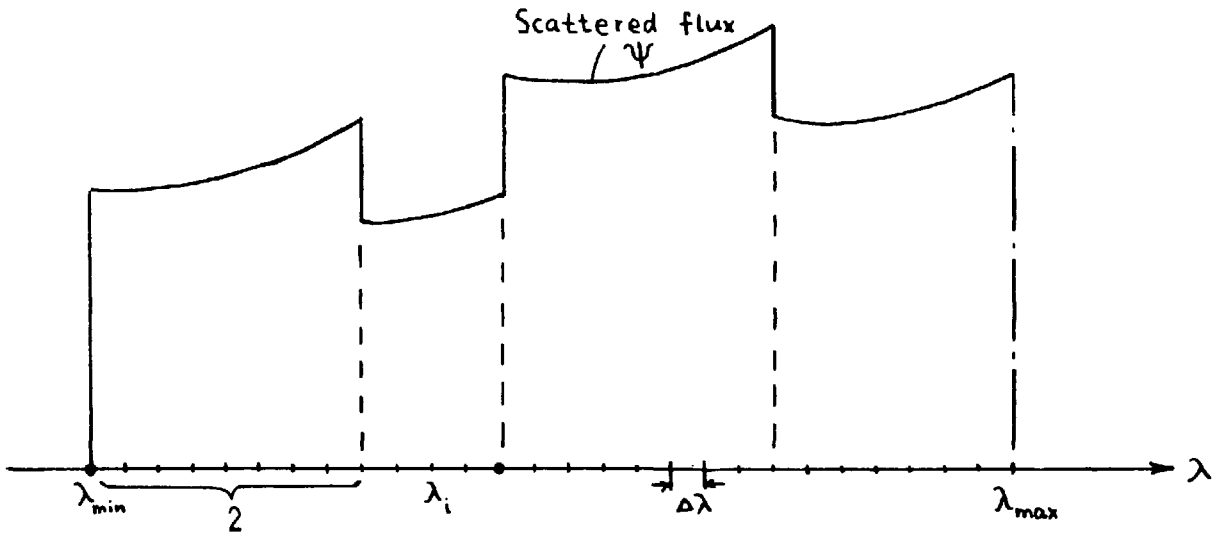

• : position of source lines (adjusted)

$$\lambda_{min} = \frac{f}{E_{max}}, \quad \lambda_{max} \simeq \frac{f}{E_{cut}}, \quad N = \frac{\lambda_{max} - \lambda_{min}}{\Delta\lambda} \ (=27), \quad m = \frac{1}{\Delta\lambda} \ (=4)$$

Fig. 2. Wavelength scale and qualitative solution for scattered flux

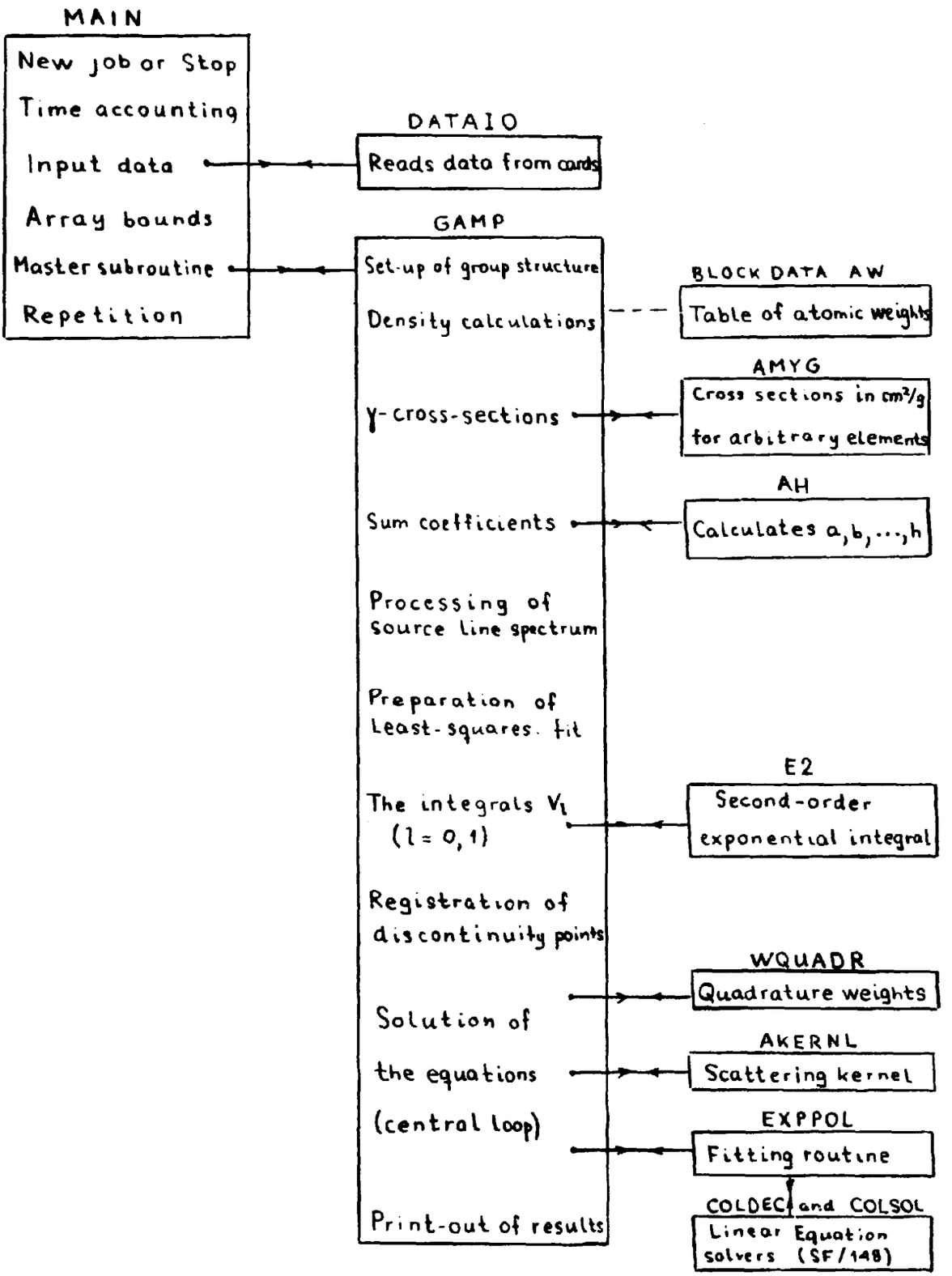

Fig. 3. Flow diagram for GAMP1

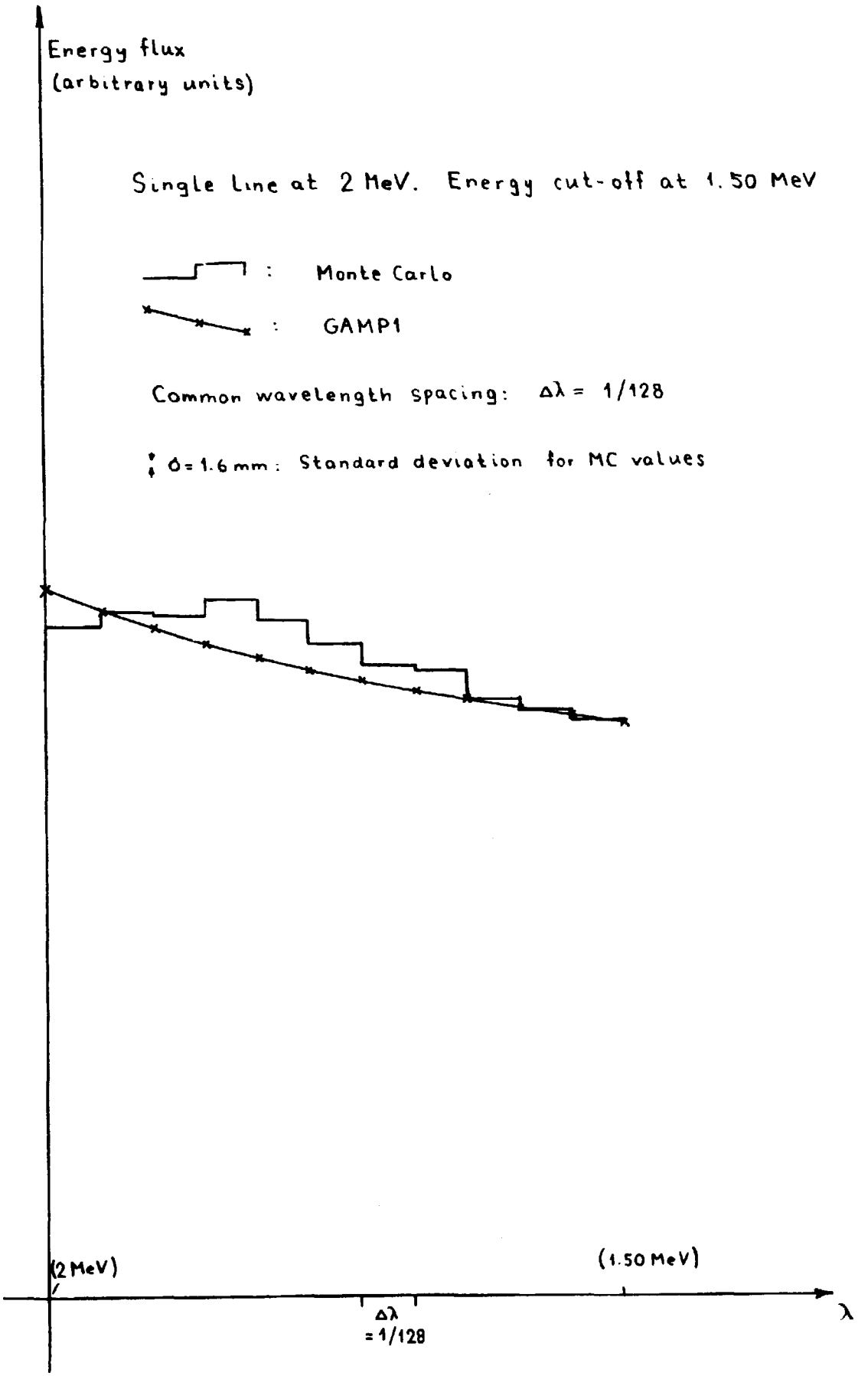

Fig 4. Comparison between double-P_1 and Monte Carlo results

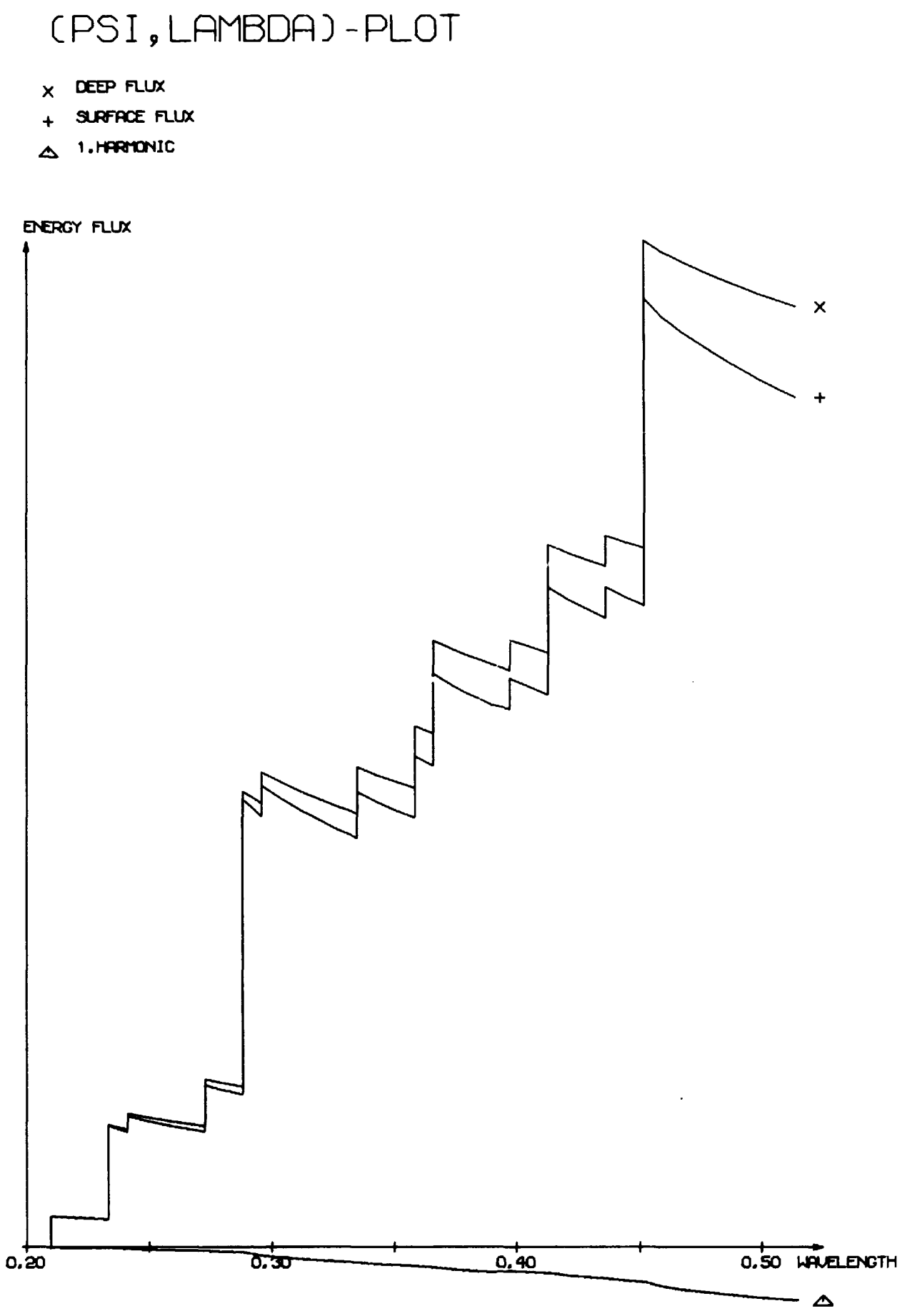

Fig. 5. Calculated scattered energy flux above concrete with nat.-U sources.

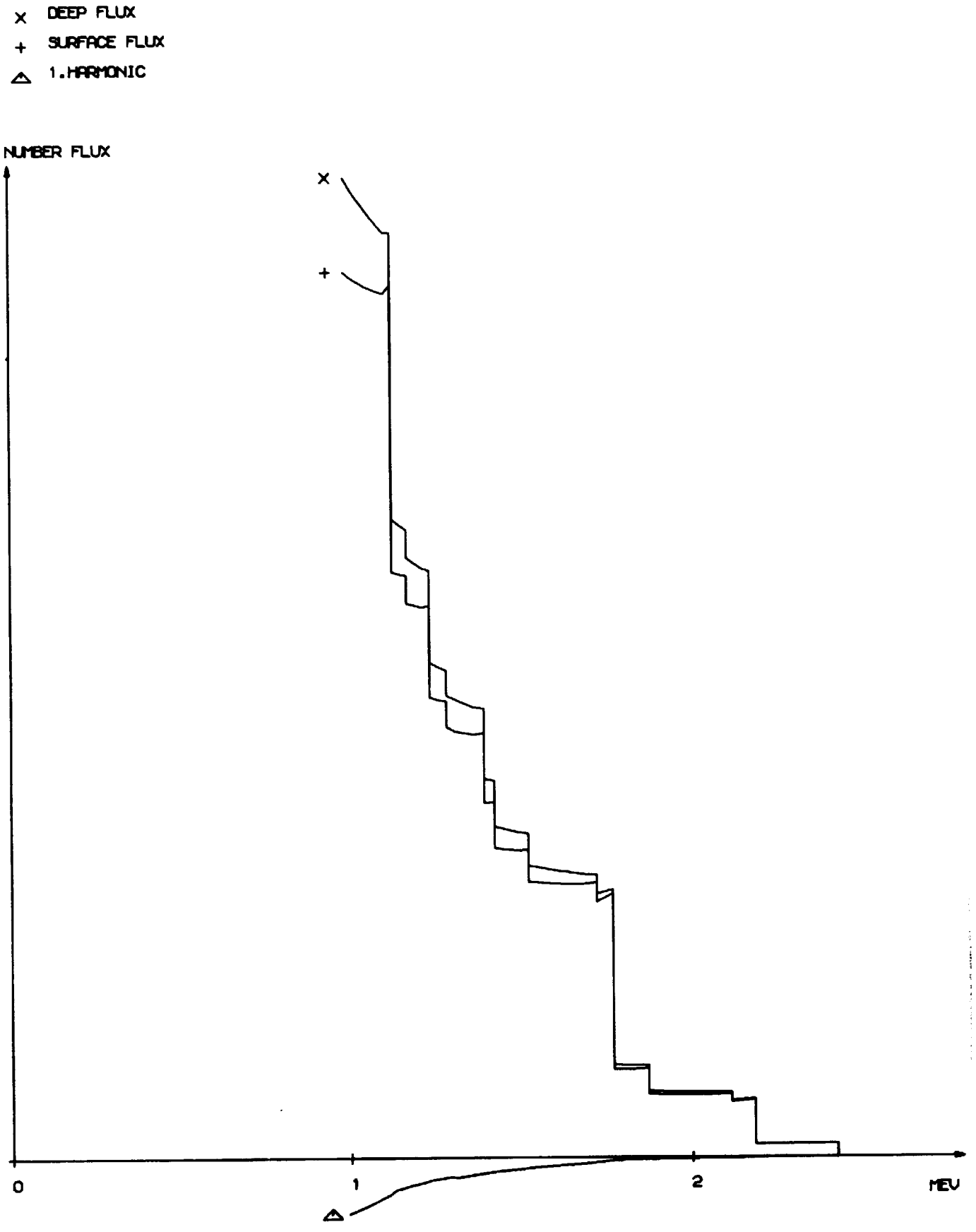

Fig. 6. Calculated scattered number flux above concrete with nat.-U sources.